A novel microRNA located in the *TrkC* gene regulates the Wnt signaling pathway and is differentially expressed in colorectal cancer specimens

Received for publication, September 27, 2016, and in revised form, January 18, 2017 Published, Papers in Press, January 18, 2017, DOI 10.1074/jbc.M116.760710

Sadat Dokanehiifard[‡], Atena Yasari[‡], Hadi Najafi[‡], Meisam Jafarzadeh[‡], Maryam Nikkhah[§], Seyed Javad Mowla[‡], and Bahram M. Soltani[‡1]

From the [‡]Department of Molecular Genetics, Faculty of Biological Sciences and [§]Department of Nano-Biotechnology, Faculty of Biological Sciences, Tarbiat Modares University, Tehran, Iran 111-14115

Edited by Xiao-Fan Wang

Tropomyosin receptor kinase C (*TrkC*) is involved in cell survival, apoptosis, differentiation, and tumorigenesis. *TrkC* diverse functions might be attributed to the hypothetical non-coding RNAs embedded within the gene. Using bioinformatics approaches, a novel microRNA named *TrkC-miR2* was predicted within the *TrkC* gene capable of regulating the Wnt pathway. For experimental verification of this microRNA, the predicted *TrkC-premir2* sequence was overexpressed in SW480 cells, which led to the detection of two mature *TrkC-miR2* isomiRs, and their endogenous forms were detected in human cell lines as well. Later, an independent promoter was deduced for *TrkC-miR2* after the treatment of HCT116 cells with 5-aza-cytidine, which resulted in differential expression of *TrkC-miR2* and *TrkC* host gene. RT-quantitative PCR and luciferase assays indicated that the *APC2* gene is targeted by *TrkC-miR2*, and Wnt signaling is up-regulated. Also, Wnt inhibition by using small molecules along with *TrkC-miR2* overexpression and TOP/FOP flash assays confirmed the positive effect of *TrkC-miR2* on the Wnt pathway. Consistently, *TrkC-miR2* overexpression promoted SW480 cell survival, which was detected by flow cytometry, MTT (3-(4,5-dimethylthiazol-2-yl)-2,5-diphenyltetrazolium bromide) assays, and crystal violate analysis. RT-qPCR analysis revealed that *TrkC-miR2* is significantly up-regulated (~70 times) in colorectal tumor tissues compared with their normal pairs. Moreover, the *TrkC-miR2* expression level discriminated grades of tumor malignancies, which was consistent with its endogenous levels in HCT116, HT29, and SW480 colorectal cancer cell lines. Finally, an opposite expression pattern was observed for *TrkC-miR2* and the *APC2* gene in colorectal cancer specimens. In conclusion, here we introduce *TrkC-miR2* as a novel regulator of Wnt signaling, which might be a candidate oncogenic colorectal cancer biomarker.

TrkC[2] (tropomyosin receptor kinase C (N_000015.9)) or neurotrophin-tyrosine kinase receptor type 3 (*NTRK3*) is a member of the Trk family of neurotrophin receptors (1). Expression of Trk family receptors in some cell types either promotes cell proliferation or differentiation (2). *TrkC* is implicated in regulation of growth and survival of many human cancer tissues, acting as an oncogene or a tumor suppressor gene, and also is inactivated by epigenetic mechanisms in colorectal cancer (CRC) (3–5).

MicroRNAs (miRNAs) are highly conserved, are 18–27 nucleotides long, and are endogenously made non-coding RNAs in many organisms (6). The complicated secondary structure of miRNA precursor (pri-miRNA) is quickly processed into 1 or more (~70) nucleotides long hairpin-structured pre-miRNA molecule(s), which is further processed into its mature form located either at the 5′ or 3′ side of the stem loop (7, 8). Mature miRNA in mammalian cells often pairs imperfectly to its target transcripts, resulting in either mRNA degradation or translation inhibition (9). Although ~55,000 miRNA genes are estimated to be encoded within the human genome (10), ~2500 human miRNAs are now registered in miRBase database. Therefore, several bioinformatics tools have been developed for prediction of novel miRNAs. This software is designed based on conservation of predicted miRNA sequence, its precursor secondary structure, stability information, and similarity of the predicted miRNA to the known miRNAs (11, 12).

Colorectal cancer is the third most common cancer worldwide with an estimated one million new cases and a half-million deaths each year (13). Irregular Wnt signaling pathway, which occurs through mutations mainly of *APC*, is a primary progression event in 90% of CRCs (14, 15). Considering the invasive nature and the cost of colonoscopic screening of CRC and also the limitation of low sensitivity of fecal occult blood test, there is a pressing need for new non-invasive biomarkers with high sensitivity and specificity to improve the diagnosis of CRC (13, 16). Recently, the discovery of miRNAs that play important

This work was supported by financial aid from Tarbiat Modares University and Iran National Science Foundation Grant 91001522. The authors declare that they have no conflicts of interest with the contents of this article.

This article contains supplemental Fig. S1–S4.

The nucleotide sequences reported in this paper have been submitted to the EMBL-EBI database under EBI accession numbers HG969187, HG969188, and HG969189.

[1] To whom correspondence should be addressed. Tel.: 98-21-82884703; Fax: 98-21-82883463; E-mail: soltanib@modares.ac.ir.

[2] The abbreviations used are: TrkC, tropomyosin receptor kinase C; CRC, colorectal cancer; miRNA, microRNA; qPCR, quantitative PCR; MTT, 3-(4,5-dimethylthiazol-2-yl)-2,5-diphenyltetrazolium bromide; SRA, Sequence Read Archive; ROC, receiver operating characteristic; PTNM, pathological tumor node metastasis; TCF, T-cell factor; LEF, lymphoid enhancer factor; oligo, oligonucleotide; MRE, miRNA recognition element.

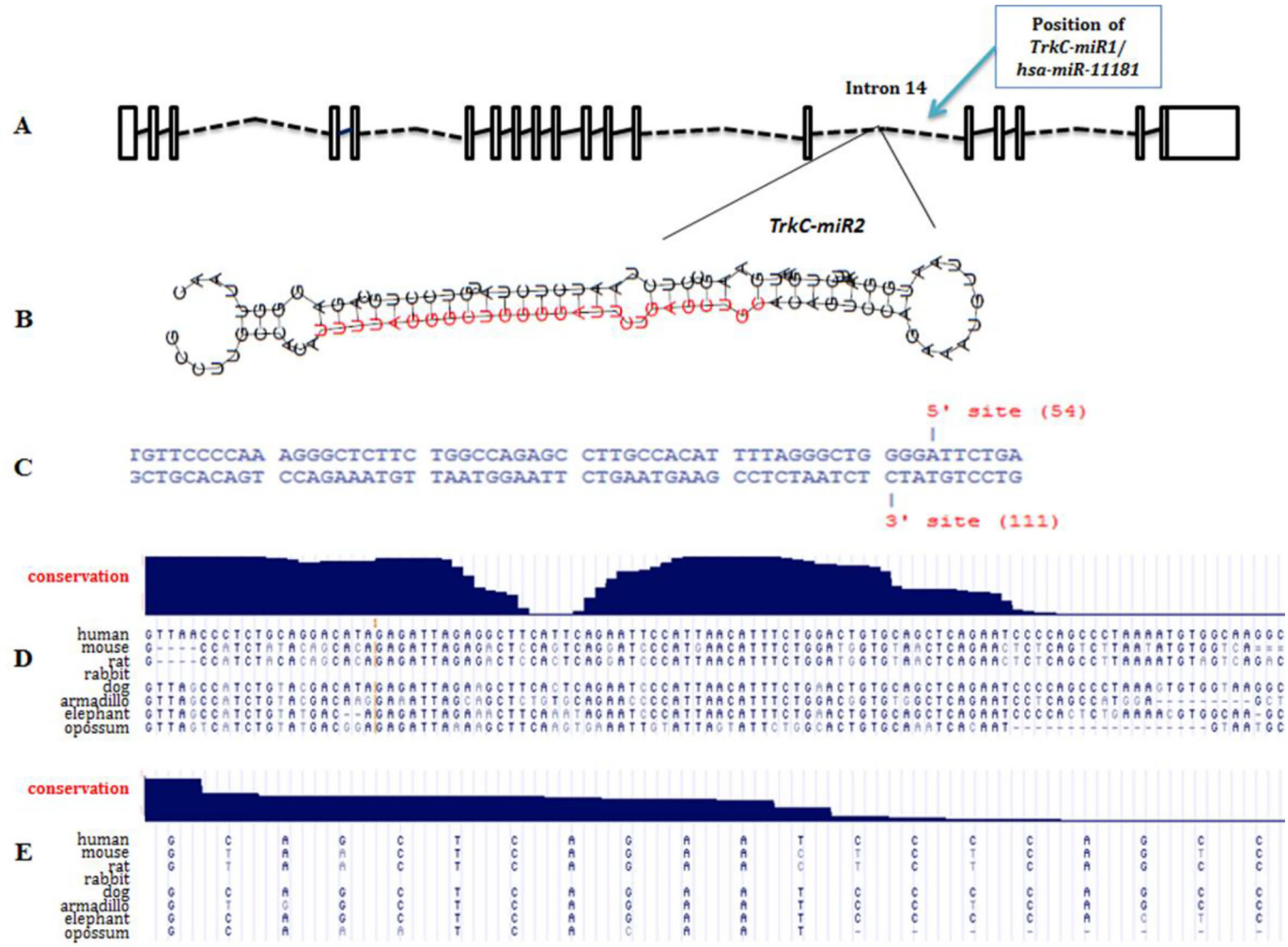

Figure 1. Bioinformatics prediction of *TrkC-miR2* encoded within the 14th intron of human *TrkC* gene. *A*, *TrkC* gene introns (*broken lines*) and exons (*rectangles*) adapted from Ensemble are shown. The position of the stem loop encoding *TrkC-miR2* is shown at in the 17-kb vicinity of the newly discovered *hsa-miR-11181*. *B*, predicted stem loop encoding *TrkC-miR2*. The *red sequence* was predicted by SSC profiler as the *TrkC-miR2* mature form. *C*, Drosha enzyme cutting sites, predicted by Microprocessor SVM tool, are shown on the sequence of hairpin structure. Blat search by the UCSC genome browser shows high conservation of *TrkC-premir2* (*D*) and *TrkC-miR2–5p* (*E*) between several organisms.

roles in oncogenesis and also in Wnt signaling regulation has opened new opportunities for the early diagnosis of CRC (13, 17, 18).

After our successful bioinformatics prediction and experimental verification of *hsa-miR-11181* (19) as the first miRNA located in *TrkC* gene, we predicted and verified *TrkC-miR2*, which is located in the vicinity of *hsa-miR-11181*. Functional analysis of the novel *TrkC-miR2* confirmed its regulatory effect on Wnt signaling pathway and suggested its potential as a CRC biomarker.

Results

Computational prediction of a novel miRNA in TrkC gene

Among 150 predicted stem loops within the introns of *TrkC* gene, one of them located in 14th intron of the gene (hg17, chr15: 86307074–86307177) and at the vicinity of *TrkC-miR1* (*hsa-miR-11181*) locus (Fig. 1*A*) had the most characteristics of a real miRNA precursor. SSC profiler predicted a *bona fide* mature miRNA sequence within this precursor (Fig. 1*B*), and Microprocessor SVM tool recognized Drosha and Dicer recognition sites in it (Fig. 1*C*). UCSC software also plotted a saddle-like pattern of conservation for the stem loop, which is a prominent characteristic of real miRNAs (Fig. 1*D*). A miRNA mature form was also conserved between mammals including dog and cat with a subtle variation of sequence compared with rodents (Fig. 1*E*). The predicted mature miRNA and its precursor were named *TrkC-miR2* and *TrkC-premir2*, respectively. Moreover, miRNA Spotter, MiRmat, Pmirp, and Mature Bayes software predicted *TrkC-miR2–5p* as *bona fide* miRNA. No identical or similar miRNA for *TrkC-miR2* has been reported in miRBase database. Alibaba2.1 Prediction Server online bioinformatics tool predicted an independent promoter for *TrkC-miR2* at ~800 bp upstream of the corresponding stem-loop, which may interact with some transcription factors including NF-κB.

Detection of exogenous and endogenous TrkC-miR2 and its sequence determination

After the overexpression of a recombinant plasmid vector containing sequences of predicted *TrkC-miR2* precursor in

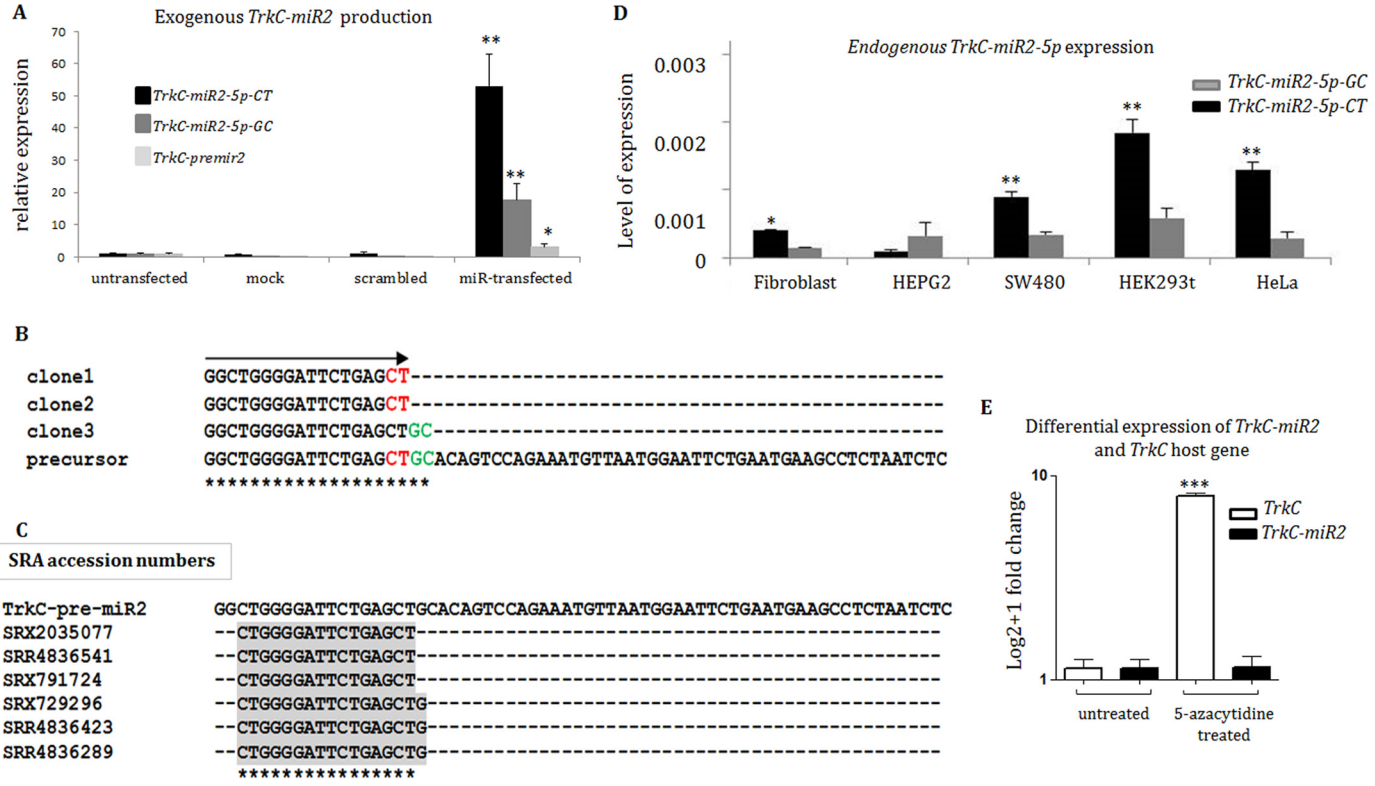

Figure 2. TrkC-miR2–5p sequence characterization and evidence for an independent promoter. *A*, overexpression of *TrkC-premir2* in SW480 cells and detection of predicted *TrkC-miR2–5p* mature forms (-CT and -GC isomiRs) by RT-qPCR. Note that *TrkC-miR2–5p-CT* isomiR is dominantly produced in the transfected cells. *B*, sequencing results of three TA vector clones containing *TrkC-miR2–5p* sequences created in *A*. *Clones 1* and *2* show the sequence of *TrkC-miR2–5p-CT* isomiR, and *clone 3* shows the sequence of *TrkC-miR2–5p-GC* isomiR. *TrkC-miR2* sequences are aligned with the sequence of their precursor. The significance of asterisks in *panels C* and *B* is the complete matching of aligned sequences at each position. *C*, shown is the presence of *TrkC-miR2* in the SRA data. Three reads for detected *TrkC-miR2-5p-CT* and *TrkC-miR2-5p-CTG* isomiRs are shown. However, no read for *TrkC-miR2-5p-GC* was detected in the SRA data set. *D*, shown is the expression level of *TrkC-miR2–5p-CT* and *-GC* isomiRs in several human cell lines. *TrkC-miR2–5p-CT* relative expression was higher than *TrkC-miR2–5p-GC* isomiR in most of these cell lines. *E*, treatment of HCT-116 cells with epidrug resulted in *TrkC* expression elevation (100 times). However, it did not have such an effect on *TrkC-miR2–5p* expression level. *Error bars* indicate S.D. of duplicate experiments. *U48* RNA and *GAPDH* were used as internal controls for the amplifications. *, $p < 0.05$; **, $p < 0.01$; ***, $p < 0.001$.

SW480 cell line, mature predicted miRNA was specifically amplified (Fig. 2*A*). When, the amplification products were cloned in the TA vector and sequenced, *TrkC-miR2–5p* sequence was represented in multiple sequencing results showing two nucleotides variation in its 3′ end, which resulted in *TrkC-miR2–5p-CT* and *TrkC-miR2–5p-GC* introduction (Fig. 2*B*). The minimum size of these sequences was submitted to the EMBL-EBI database, accessible by EBI accession numbers HG969187, HG969188, and HG969189 for *TrkC-miR2–5p-CT*, *TrkC-miR2–5p-GC*, and *TrkC-premir2*, respectively. In several RNA-sequencing data (NCBI-SRA) analysis attempts, multiple reads were detected showing *TrkC-miR2–5p-CT* expression, whereas no read was found for *TrkC-miR2–5p-GC.* Instead, several reads were detected in which the miRNA sequence was one nucleotide smaller than *TrkC-miR2*-5p-GC, meaning one nucleotide longer than *TrkC-miR2–5p-CT*. This may suggest a novel *TrkC-miR2* isomiR (Fig. 2*C*). Endogenous *TrkC-miR2* expression was also detected in HEPG2, SW480, HEK293t, HeLa, and fibroblast human cell lines through RT-qPCR (Fig. 2*D*). The highest expression level of *TrkC-miR2* was detected in HEK293t cells, and the *TrkC-miR2–5p-CT* level was higher than *TrkC-miR2–5p-GC* isomiR in most of these cell lines (Fig. 2*D*).

Evidence for an independent promoter for TrkC-miR2

The HCT-116 cell line was treated with 5-azacytidin epidrug, and the expression levels of *TrkC-miR2* and *TrkC* were measured and compared with the levels of these genes in untreated HCT-116 cells. RT-qPCR results indicated that the *TrkC* expression level has been elevated up to 100 times in the epidrug-treated cells compared with the untreated ones. However, *TrkC-miR2*-5p expression level was not affected by epidrug treatment (Fig. 2*E*).

Direct interaction of TrkC-miR2 with APC2–3′-UTR

~700 target genes were predicted for *TrkC-miR2*-5p using Dianna lab software. *APC2* (ENSG00000115266) gene was the highest scored target gene in which 23 highly conserved *TrkC-miR2*-5p-specific MREs were predicted in its 3′-UTR. A DNA fragment containing the *TrkC-miR2* precursor was PCR-amplified from the human genome and cloned in fusion with GFP/ORF in the pEGFP-C1 expression vector. Then, RT-qPCR indicated significant down-regulation (60%) of the *APC2* expression level in the SW480 cells transfected with *TrkC-miR2* precursor (Fig. 3*A*). When 3′-UTR sequence of *APC2* was cloned downstream of Renilla luciferase ORF and co-expressed with *TrkC-miR2* in HEK293t cells, a dual luciferase assay sup-

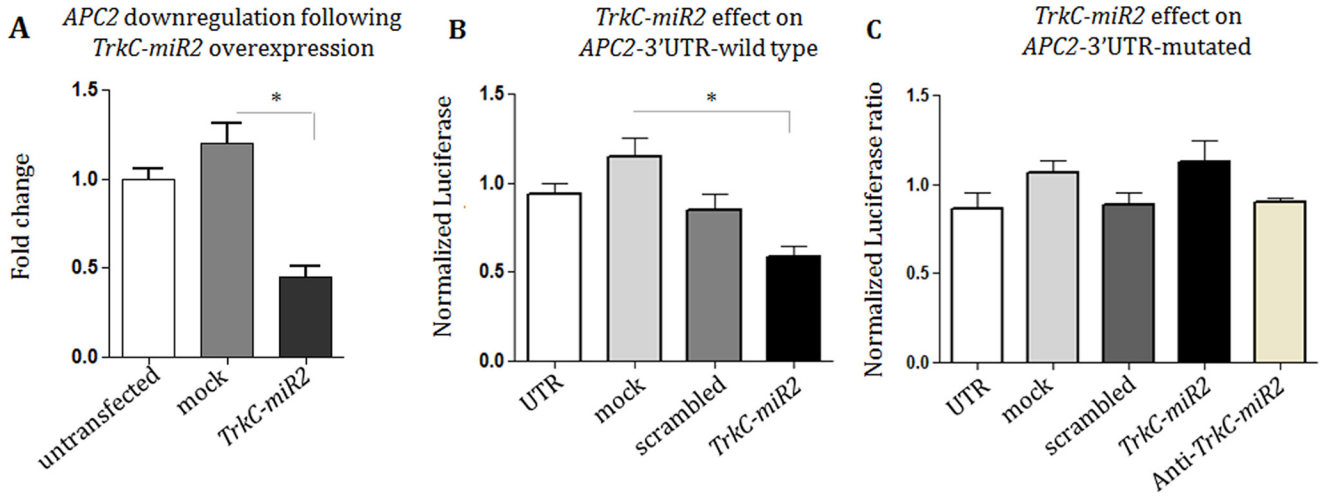

Figure 3. TrkC-miR2 direct interaction with its predicted target gene. *A*, RT-qPCR result shows *APC2* gene down-regulation after *TrkC-premir2* overexpression in the SW480 cell line compared with the related controls. *B*, dual luciferase assay supported *TrkC-miR2* direct interaction with 3′-UTR sequence of *APC2* target gene. *C*, lack of interaction between the overexpressed *TrkC-miR2* and mutated *APC2,3′*-UTR detected by dual luciferase assay and supported direct interaction between this miRNA and the wild-type sequence of APC2,3′-UTR sequence shown in *B*. *, $p < 0.05$.

ported direct interaction with *APC2* transcript, showing 55% reduction in luciferase count (Fig. 3*B*). When, mutated *APC2*, 3′-UTR (supplemental Fig. 1) was used in the same experiment, and *TrkC-miR2* overexpression did not significantly change the luciferase expression level (Fig. 3*C*). Co-expression of *TrkC-miR2* with cassettes containing *APC* (supplemental Fig. 2*A*), *AxinI* (supplemental Fig. 2*B*), and *AxinII* (supplemental Fig. 2*C*) 3′-UTRs sequences downstream of Renilla luciferase ORF showed no significant alteration of Renilla luciferase activity compared with mock or scrambled controls.

TrkC-miR2 as a novel regulator of Wnt signaling in SW480 cells

TrkC-miR2 overexpression effect on the Wnt signaling pathway was investigated through TOP/FOP flash assay. To this aim, Wnt signaling positive SW480 cells was transiently co-transfected using pGL4-TOP and *TrkC-miR2*-overexpressing vectors, and results were compared with the situation that pGL4-TOP was co-transfected with scrambled or mock recombinant vectors. Luciferase activity in the SW480-TOP cells overexpressing *TrkC-miR2* was significantly increased (~2-fold, $p < 0.05$) compared with the mock and scrambled negative vectors. For the reporter assay, relative luciferase activities of SW480-TOP cells were strongly higher than those of SW480-FOP cells (Fig. 4*A*).

The effect of *TrkC-miR2* overexpression on the Wnt signaling pathway was further investigated through RT-qPCR analysis against downstream genes of the pathway. The expression level of the genes involved in canonical and non-canonical Wnt signaling pathways (*c-MYC*, *CCND1*, *AxinI*, *APC1*, *B-catenin*, and *TNFα*) was significantly elevated after *TrkC-miR2* overexpression in SW480 cell line (Fig. 4*B*).

SW480 cells were also treated with XAV932 (increases *AxinI* expression), PNU74654 (inhibits β-catenin and TCF interaction), and IWP-2 (inhibits LRP) small molecules in order to manipulate Wnt signaling pathway at different steps. Then, these cells were co-transfected with pGL4-TOP and *TrkC-miR2*-overexpressing vectors, and results were compared with the situation that pGL4-TOP was co-transfected with scrambled or mock constructs. Luciferase activity in SW480-TOP cells, which were treated with XAV932 and IWP-2, was significantly increased when *TrkC-miR2* was overexpressed compared with the mock and scrambled negative vectors ($p < 0.05$). However, when β-catenin and TCF interaction was inhibited by using PNU74654, overexpression of *TrkC-miR2* did not significantly change the Wnt signaling (Fig. 4*C*).

Using anti-*TrkC-miR2*, this miRNA was significantly down-regulated in SW480 cells (Fig. 4*D*), which was followed by the elevation of *APC2* gene expression (Fig. 4*E*) and non-significant reduction of the Wnt activity (Fig. 4*F*). Scavenging of *TrkC-miR2* through overexpression of *APC2*-3′-UTR (Fig. 4*D*) also resulted in elevation of *APC2* gene expression (Fig. 4*E*) and also non-significant reduction of Wnt activity (Fig. 4*F*). Mock and *HBEGF*-3′-UTR constructs were applied as controls.

Although the overexpression of *TrkC-premiR2* in HUH7 cells (Fig. 4*G*) resulted in significant down-regulation of *APC2* gene expression (Fig. 4*H*), it was not effective on the Wnt signaling activity (Fig. 4, *I* and *J*).

Up-regulated TrkC-miR2 in CRC-originated cell lines and tissue samples

Endogenous expression of *TrkC-miR2–5p-CT* was detected through RT-qPCR in low (HT29), intermediate (HCT-116), and high (SW480) grades of human colon cancer cell lines. The highest expression level of *TrkC-miR2–5p-CT* was detected in SW480 cell line; however, the minimum expression level of it was detected in the HT29 cell line (Fig. 5*A*).

TrkC-miR2

5p-CT was detected in 36 colorectal cancer sample pairs, whereas *TrkC-miR2-5p-GC* expression was not detected. *TrkC-miR2–5p-CT* was ~70-fold up-regulated in tumor tissues compared with the paired adjacent non-tumor samples ($p < 0.0001$) (Fig. 5*B*), which was supported with Mann-Whitney analysis (Fig. 5*C*). CRC tumor samples were distributed in all four grades (1–4). These data showed significant differences between different grades of malignancy (Fig. 5*D*). Although

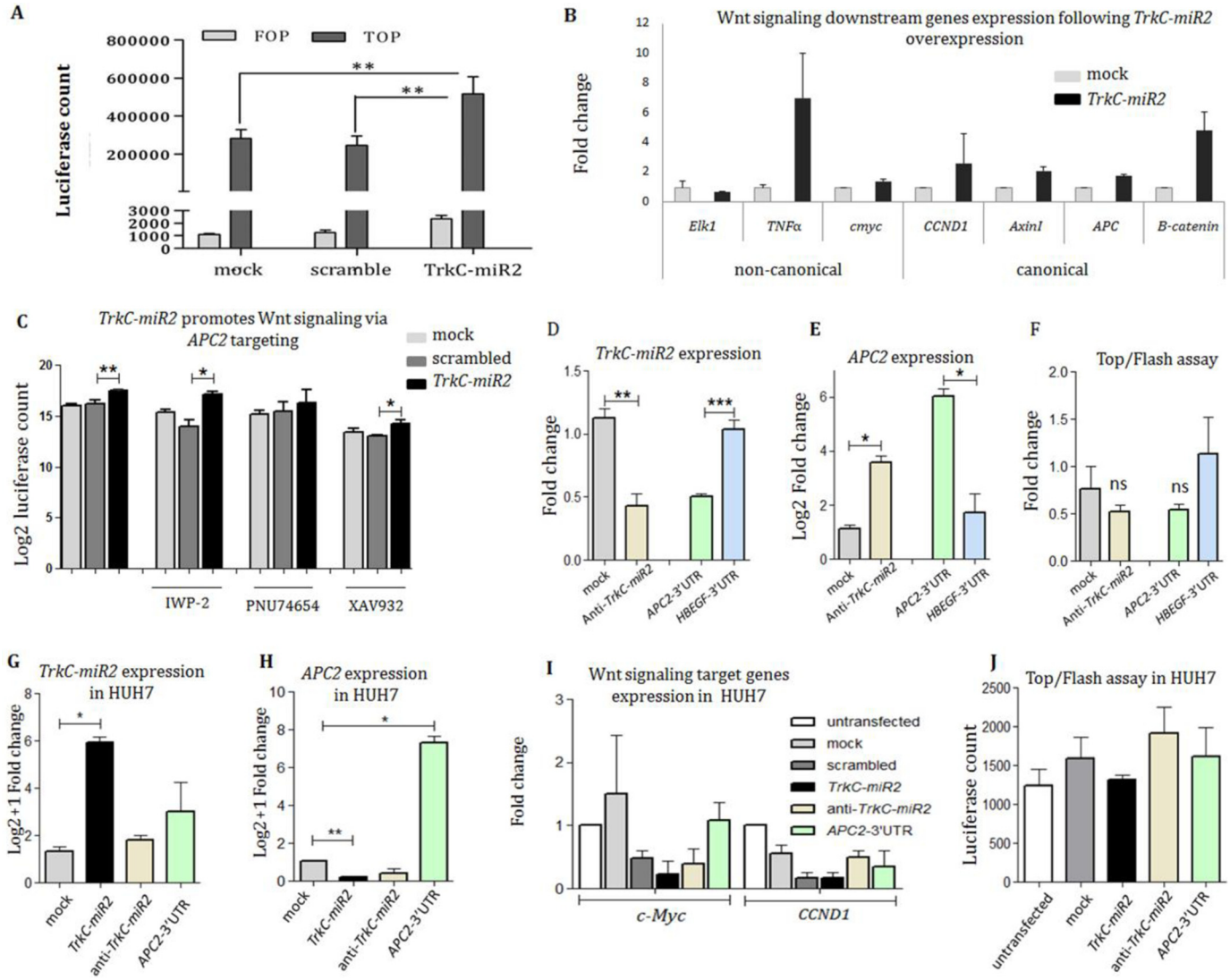

Figure 4. TrkC-miR2 expression alteration effect on the Wnt signaling pathway. *A*, Wnt signaling up-regulation after *TrkC-miR2* overexpression in the SW480 cells. Luciferase activity was significantly increased in the cells overexpressing *TrkC-premir2* compared with the controls. *B*, increased expression level of the genes involved in both canonical and non-canonical Wnt signaling pathway after *TrkC-miR2* overexpression. *C*, Wnt inhibitor small molecules and *TrkC-miR2* co-treatment effect on the Wnt signaling is shown through Top/flash assay. Although Wnt signaling is down-regulated after the XAV932 and IWP-2 small molecules application, this down-regulation has been compensated by *TrkC-miR2* overexpression compared with the controls. When the cells were treated with the PNU74654 small molecule, significant Wnt signaling alteration was not detected with or without *TrkC-miR2* overexpression. *Error bars* indicate S.D. of three experiments. *D*, successful down-regulation of *TrkC-miR2* using *anti-TrkC-miR2* sequence in SW480 cells (compared with the mock control). Also, *APC2-3′*-UTR overexpression as a scavenger, resulted in down-regulation of *TrkC-miR2* (compared with the non-scavenger *HBEGF*-3′-UTR sequence), detected by RT-qPCR. Expression data were normalized against *U48* as an internal control. *E*, RT-qPCR results showed significant up-regulation of *APC2* expression after the down-regulation of *TrkC-miR2* (using *anti-TrkC-miR2*) or after the scavenging of *TrkC-miR2* (by *APC2*-3′-UTR overexpression) in SW480 cells. Expression data were normalized against *GAPDH* as an internal control. *F*, top/Fop flash assay after transfection of anti-*TrkC-miR2* in SW480 cells showing non-significant Wnt signaling reduction compared with the mock transfected control. Also, overexpression of *APC2*-3′-UTR as a *TrkC-miR2* scavenger again resulted in non-significant Wnt signaling attenuation compared with the off-target *HBEGF*-3′-UTR overexpression. *ns*, not significant. *G*, RT-qPCR analysis of *TrkC-miR2* expression in HUH7 cell lines after *TrkC-premiR2*, anti-*TrkC-miR2*, and *APC2*-3′-UTR overexpression compared with mock control. *TrkC-miR2* level was significantly increased in the cells overexpressing *TrkC-premiR2*; however, anti-*TrkC-miR2* and *APC2*-3′-UTR scavenger constructs were not capable of significant reduction in *TrkC-miR2* level. *H*, shows *APC2* expression alteration after *TrkC-premiR2*, anti-*TrkC-miR2*, and *APC2*-3′-UTR overexpression. *APC2*-3′-UTR-specific primers were used for detection of *APC2* expression alteration. Only successful overexpression of *TrkC-miR2* (*G*) has resulted in significant reduction of *APC2* transcripts. *I*, RT-qPCR against *c-Myc* and *CCND1* genes (as the Wnt signaling target genes) after the overexpression of interested constructs. Data indicate no significant Wnt signaling alteration after the *TrkC-miR2* expression alteration in Huh7 cells. *J*, shown is the Top/flash assay in the HUH7 cell line before and after *TrkC-miR2* expression alteration. Similar to *I*, no significant Wnt signaling alteration was detected. *, $p < 0.05$; **, $p < 0.01$; ***, $p < 0.001$.

TrkC-miR2 expression was not significantly altered between the tumors at stages of 2–4 (Mann-Whitney test, $p > 0.05$), a non-significant steady/gradual increase of *TrkC-miR2* expression was detected during the increase of CRC stages ($p < 0.005$) (Fig. 5*E*).

To investigate the suitability of *TrkC-miR2-5p-CT* for discrimination of tumor *versus* non-tumor states of CRC samples, sensitivity and specificity were calculated using ROC (receiver operating characteristic) curve analysis. An area under the curve = 0.79 for *TrkC-miR2-5p-CT* (p value = 0.0001; Fig. 5*F*) was calculated, which is a score greater than the cutoff (0.7) needed for a considerable biomarker. The expression levels of *TrkC-miR2* and *APC2* were compared in >20 individuals tumor samples showing a significant negative correlation

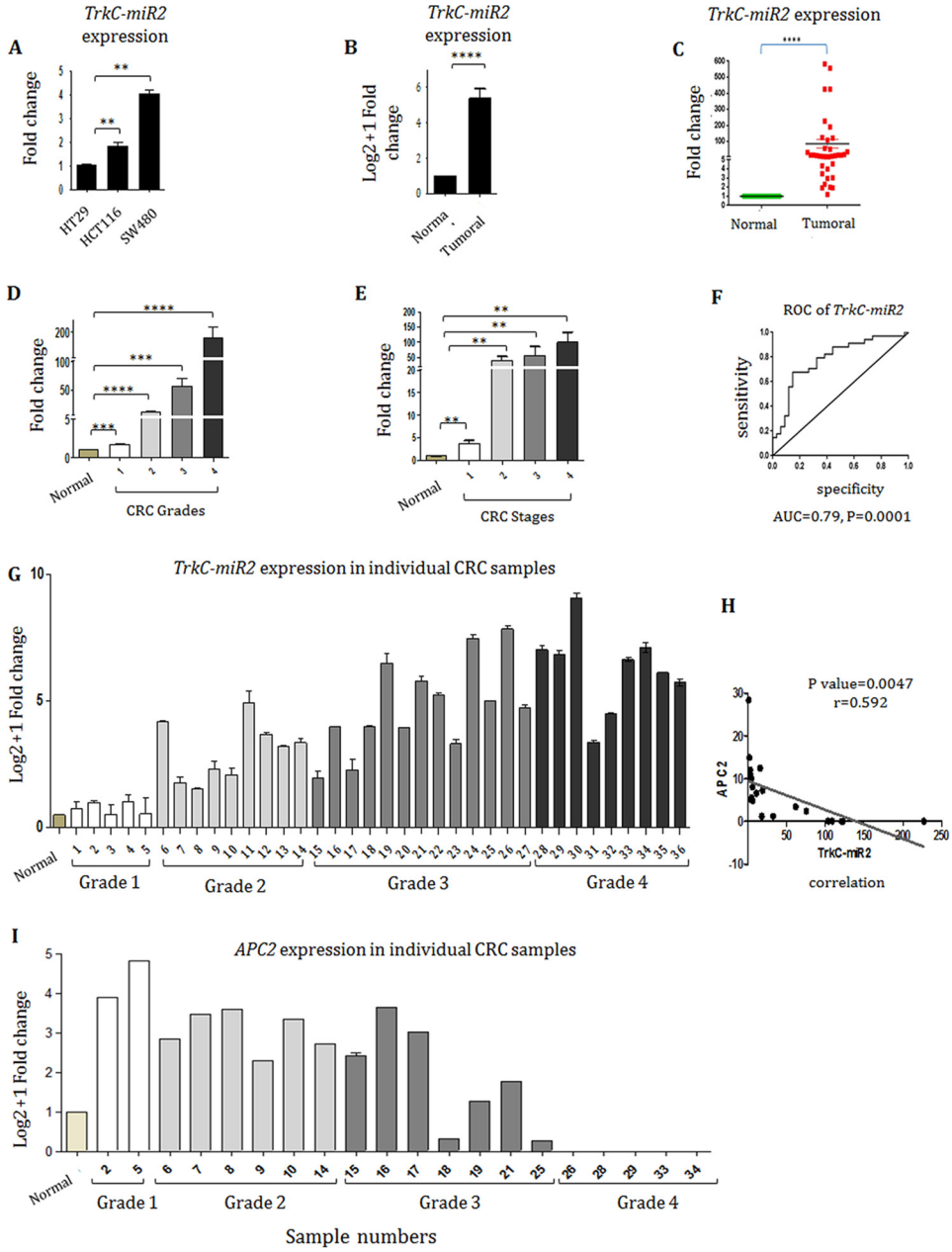

Figure 5. Implication of *TrkC-miR2* in colorectal cancer. *A*, *TrkC-miR2*-5p-CT expression level in HCT-116 and SW480 cells was 2- and 4-fold higher than HT29 cell line ($p < 0.005$), respectively. *B*, *TrkC-miR2* expression status in 36 CRC tumor (*T*) tissues and normal (*N*) pairs. *C*, Mann-Whitney analysis indicated that *TrkC-miR2* has been significantly increased in CRCs (~70-fold) compared with the paired adjacent non-CRC tissue samples ($p < 0.0001$). *D*, increased expression of *TrkC-miR2* detected in the more advanced grades of CRCs compared with the normal ones ($p < 0.001$). *E*, *TrkC-miR2* expression in different stages of CRC samples. *Error bars* indicate S.E. of tetraplicate experiments. *F*, ROC curve analysis of *TrkC-miR2* expression in CRC patients. The up-regulated *TrkC-miR2* expression yielded an area under the curve (*AUC*) value of 0.79 (95% confidence interval: 0.6714–0.8944) with 75% sensitivity and 75% specificity, supported *TrkC-miR2* expression as a diagnostic value for discriminating CRC from healthy controls. *G*, *TrkC-miR2* expression analysis in individual samples, distributed in high and low grade samples. Samples are shown by the numbers. *H*, a significant negative correlation was calculated between *TrkC-miR2* and *APC2* expression with a correlation coefficient (*r*) of −0.592 and a significant *p* value of 0.0046. *I*, *APC2* expression analysis in individual high and low grade samples. *Error bars* indicate S.D. of duplicated experiments. *, $p < 0.05$; **, $p < 0.01$; ***, $p < 0.001$; ****, $p < 0.0001$.

between them with a correlation coefficient (r) of −0.592 ($p = 0.0046$) (Fig. 5, *G–I*).

Survival effect of TrkC-premir2 overexpression in SW480 cell line

SW480 and HUH7 cell lines were transfected using *TrkC-premir2*-overexpressing vector, and cell cycle distribution of the cells was examined (Fig. 6). No significant sub-G_1 population alteration was detected in HUH7 cells overexpressing *TrkC-premir2* compared with the control cells (Fig. 6*A*). However, overexpression of *TrkC-premir2* in SW480 cells rendered a significant reduction in sub-G_1 cell population compared with the negative control. Knockdown of this miRNA did not significantly alter the subG_1 population rate (Fig. 6*B*). Consistently, an MTT assay (Fig. 6*C*) and crystal violet analysis (Fig. 6*D*) indicated no significant proliferation rate alteration in the transfected HUH7 cells overexpressing *TrkC*-premir2 compared with the related control cells. Furthermore, overexpres-

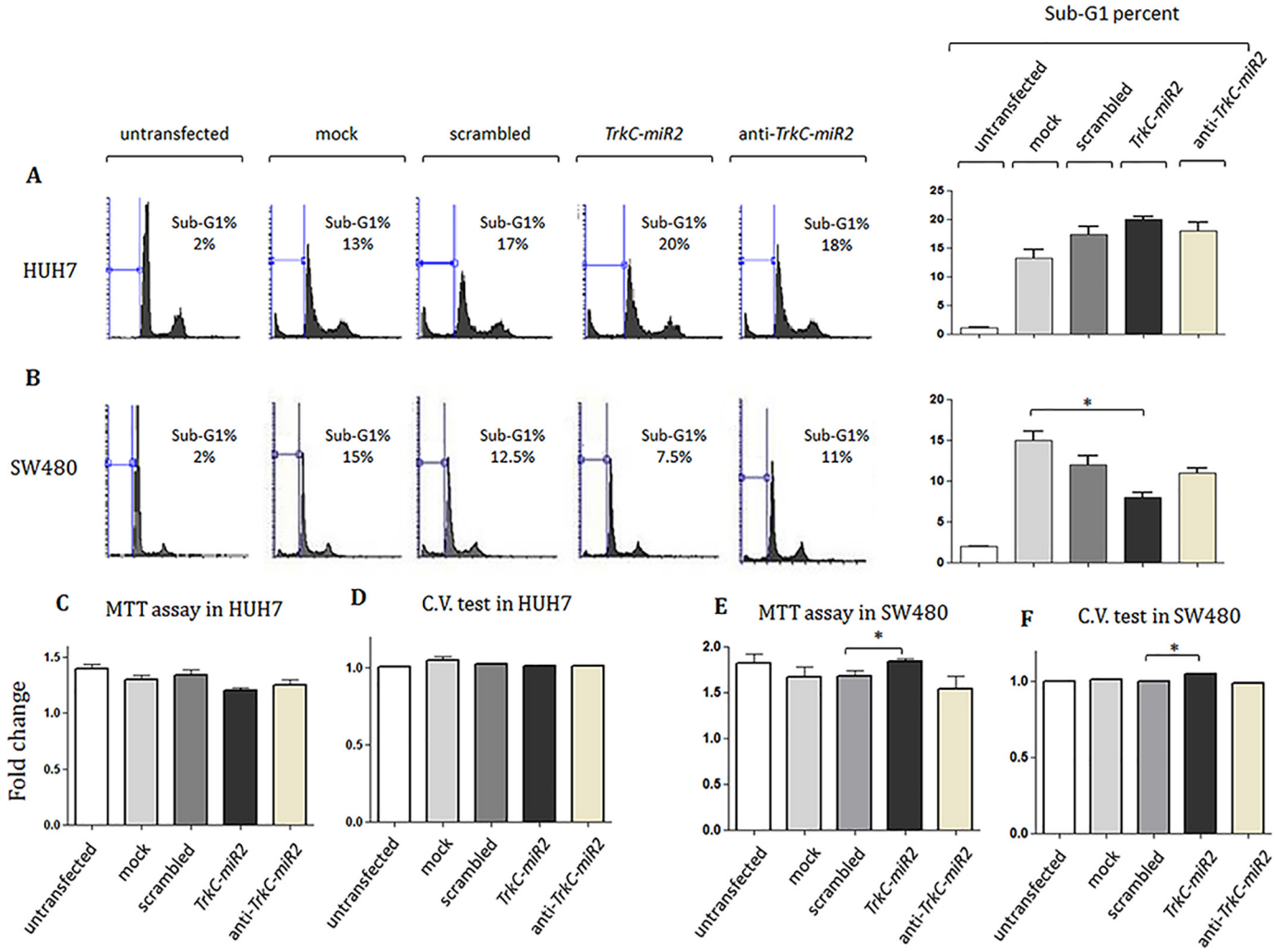

Figure 6. Cell cycle and survival analysis for the cells overexpressing *TrkC-premir2*. *A* and *B*, shown is flow cytometry propidium iodide staining 36 h after transfection of two different cell lines in which *TrkC-premir2* has been overexpressed or down-regulated. Although no significant alteration was detected for HUH7 cell line (*A*), *t* test analysis indicated a significant reduction in sub-G_1 cell cycle distribution of SW480 (*B*)-transfected cells after *TrkC-miR2* overexpression. However, knockdown of *TrkC-miR2* in both cell types did not significantly change the sub-G_1 percentages of the cells. *C* and *D*, MTT and crystal violet assay against HUH7 cells under *TrkC-miR2* expression alteration. No significant cell survival alteration rate was calculated in these situations. *E* and *F*, MTT and crystal violet assay against SW480 cells under *TrkC-miR2* expression alteration. A significant cell survival alteration rate was calculated when *TrkC-miR2* was overexpressed. *, $p < 0.05$

sion of *TrkC-premir2* in SW480 cells resulted in significant elevation of survival rate detected by both MTT (Fig. 6*E*) and crystal violet assays (Fig. 6*F*) compared with the negative control.

Discussion

miRNAs are known to be involved in many processes including cancer and differentiation (20). Because their discovery through forward genetics is relatively inefficient (21), bioinformatics tools are established for prediction of novel miRNAs (22). TrkC receptor is known to be involved in neurotrophin signaling, which is related to cell death, survival, cancer, and differentiation, similar to Wnt signaling (3, 5, 23–25). On the other hand *TrkC* is a potential tumor suppressor gene commonly inactivated by epigenetic mechanisms in CRC (3, 5). Despite its widespread involvement in cell signaling, molecular mechanisms that regulate Wnt signaling pathway are poorly understood (26). Hence, discovery of common regulatory factors for the Wnt signaling pathway may provide the possibility of cell fate manipulation in the cases of diseases like CRC and tissue regeneration. Our previous attempts resulted in discovery of *hsa-miR-6165* (27) and *hsa-miR-11181* (19), which are located in *NGFR* and *TrkC* genes, respectively. Herein, we gathered bioinformatics and supportive experimental evidences showing the presence of a second novel miRNA located in the *TrkC* gene that has the potential of being considered as a regulator of Wnt signaling pathway and also has the potential to be used as a valuable biomarker for diagnosis of CRC.

Detection of TrkC-miR2 that is driven by an independent promoter

One of the *bona fide* predicted stem loops in *TrkC* intron 14th (Fig. 1*A*), named *TrkC-premir2*, showed the most criteria for producing novel *TrkC-miR2* (Fig. 1*B*). A Drosha processing site was predicted in *TrkC-premir2* (Fig. 1*C*), and like most of known miRNAs precursors (12), a saddle-like conservation plot was predicted for it (Fig. 1*D*). *TrkC-miR2* is conserved in mam-

mals like dog and cat (Fig. 1*E*), and no identical sequence has been reported for *TrkC-miR2* in the miRBase database.

Similar to the approaches used by others (19, 27, 28), exogenous production of mature *TrkC-miR2* was detected when a DNA fragment corresponding to *TrkC-premir2* sequence was overexpressed in SW480 cells (Fig. 2*A*). Then, production of mature *TrkC-miR2* was confirmed by sequencing of specifically amplified RT-qPCR products (Fig. 2*B*). Interestingly, similar to many other reported miRNAs (29–31), *TrkC-miR2–5p-CT* and *TrkC-miR2–5p-GC* isomiRs were processed from the 5′ arm of its precursor. Next generation sequencing (NGS) data analysis revealed the existence of several reads for *TrkC-miR2–5p-CT*, which once again supported the identity of this miRNA. Also, there was no SRA (Sequence Read Archive) read for *TrkC-miR2–5p-GC* consistent with the lower expression level we have detected for this isomiR compared with the level of *TrkC-miR2–5p-CT*. Interestingly several SRA reads were found containing one nucleotide longer than *TrkC-miR2–5p-CT*, which could be considered as another *TrkC-miR2* isomiR (Fig. 2*C*). Endogenous production of these isomiRs was confirmed in several cell lines in which *TrkC-miR2–5p-CT* expression level was higher than *TrkC-miR2–5p-GC* isomiR (Fig. 2*D*).

Differential expression of *TrkC* and *TrkC-miR2* in different tumor samples (data not shown) suggested an independent promoter for this miRNA in *TrkC* gene sequences. Further evidence for the presence of an independent promoter came from HCT-116 cells treated with 5-azacytidine epidrug (3, 5). By default, *TrkC* gene is expressed in a very low level as a result of promoter methylation in HCT-116 cells (5). *TrkC* gene expression level was increased 100 times in the HCT-116 cells treated with 5-azacytidine, whereas *TrkC-miR2–5p* expression was not altered before and after 5-azacytidine treatment (Fig. 2*E*). Overall, accumulative evidence supported the presence of two or maybe three isomiRs for the novel *TrkC-miR2*, which is driven by an independent promoter.

Association between TrkC-miR2 and Wnt signaling pathway

APC2 as a major Wnt signaling pathway component was predicted as the highest scored target gene for *TrkC-miR2–5p*. Therefore, *TrkC-premir2* was overexpressed in SW480 cells, and RT-qPCR results indicated that the *APC2* transcription level has been down-regulated in these cells (Fig. 3*A*). Furthermore, a dual luciferase assay supported direct interaction of *TrkC-miR2* with the wild-type sequence of *APC2*, 3′-UTR (Fig. 3*B*), whereas it did not have a similar effect on the mutated *APC2*, 3′-UTR sequence (Fig. 3*C*). Meanwhile, *TrkC-premir2* overexpression did not show such an effect on the other tested Wnt signaling pathway components (supplemental Fig. 2). These results suggested *TrkC-miR2* as a novel regulator that affects the Wnt signaling pathway inhibitory complex only through *APC2* gene expression, and further analysis in physiological condition was needed to confirm its function.

During Wnt signaling, Wnt ligands interact with Frizzled and LRP co-receptors leading to inactivation of the tumor suppressive genes *APC*, *GSK-3β*, and *Axin* and finally release β-catenin oncogenic protein (32). After nuclear translocation of β-catenin, which complexes with TCF/LEF transcription factors, Wnt-responsive genes such as CyclinD1 (*CCND1*) is up-regulated, and cell cycle is motivated (33).

APC2 as a negative regulator of Wnt signaling pathway (26) was shown to be targeted by *TrkC-miR2* (Fig. 3). Also, overexpression of *TrkC-miR2* resulted in Wnt signaling up-regulation (Fig. 4, *A* and *B*). Therefore, it was interesting to know if the effect of this novel miRNA is confined to the *APC2* transcripts. To do so, Wnt signaling was blocked via small molecules at three points of this pathway, and then activity of the pathway was measured through TOP/FOPflash assay system after *TrkC-miR2* overexpression. When *TrkC-miR2* was overexpressed in SW480 cells that were treated with IWP-2 small molecule (inhibitor of LRP receptor) (34), Wnt signaling was up-regulated compared with the cells that were treated with this small molecule as well as mock and scrambled controls (Fig. 4*C*). That means *TrkC-miR2* effect is downstream to the LRP receptor in the Wnt signaling pathway. When *TrkC-miR2* was overexpressed in the SW480 cells that were treated with PNU74654 (inhibits β-catenin and TCF interaction; Refs. 35 and 36), Wnt signaling was not significantly affected compared with the cells that were co-treated with this small molecule as well as control vectors (Fig. 4*C*). This result once again emphasizes that *TrkC-miR2* works upstream to the β-catenin where the APC2 protein does its function. When *TrkC-miR2* was overexpressed in the SW480 cells that were treated with XAV932 (up-regulates *AxinI* expression and down-regulates Wnt signaling; Refs. 37 and 38), the result was an elevation of Wnt signaling consistent with its down-regulation effect on *APC2* expression (Fig. 4*C*). This experiment again introduces *TrkC-miR2* as a positive regulator of Wnt signaling pathway, potentially via targeting of *APC2*. Finally, using antisense against the *APC2* gene expression, the *APC2* gene was successfully down-regulated, and then *TrkC-miR2* overexpression no longer had a significant effect on the Wnt signaling activity (supplemental Fig. 4).

Although *TrkC-miR2* was down-regulated and *APC2* was up-regulated after the application of anti-*TrkC-miR2* or *APC2*-3′-UTR scavenger constructs in SW480 cells, the expected Wnt signaling attenuation was not significant (Fig. 4, *D–F*). This might be justified by the suggestion of a saturation status for Wnt signaling inhibitory complex in which APC2 protein is a component along with APC, GSK3, and Axin proteins.

The expression level of *TrkC-miR2* in HUH7 cells was much lower (1/100) than its level in SW480 cells detected by RT-qPCR (supplemental Fig. 3*A*). Therefore, it may justify that down-regulation of *TrkC-miR2* in HUH7 cells (Fig. 4*G*) was not as efficient as in SW480 cells (Fig. 4*D*).

Successful overexpression of *TrkC-miR2* in HUH7 cells (Fig. 4*G*) was also followed by down-regulation of the *APC2* target gene (Fig. 4*H*), but it was not capable of affecting Wnt signaling (Fig. 4, *I* and *J*), unlike in SW480 cells (Fig. 4, *A* and *B*). This might be justified by lower Wnt activity in HUH7 cells. RT-qPCR indicated a 6000× higher *APC2* expression level in HUH7 cells compared with SW480 cells (supplemental Fig. 3*B*). That means, although *TrkC-miR2* overexpression has resulted in *APC2* down-regulation, its level still has been too high to allow Wnt signaling up-regulation. Consistently, Top/flash assay counts (relative light units) compared with SW480 and HUH7 cells indicate that Wnt activity in HUH7 cells is much

lower than in SW480 cells (Fig. 4, *A* and *J*). A similar low count for Wnt activity in HUH7 cells has been reported elsewhere (39). Overall, higher *APC2* gene expression levels along with lower *TrkC-miR2* levels in HUH7 cells compared with SW480 may justify the differential effect of *TrkC-miR2* overexpression in these cell lines.

Differential expression of TrkC-miR2 in CRCs and marginal non-tumor tissue samples

Wnt signaling is generally activated in CRCs (14, 15, 40), and this pathway was activated after *TrkC-miR2* overexpression followed by *APC2* reduction in SW480 cell lines (Figs. 3 and 4). Therefore, *TrkC-miR2* expression level was investigated in HT29, HCT-116, and SW480 cell lines, which originated from grades 1–3 of CRC tumors, respectively (41, 42). Results indicated that the *TrkC-miR2* expression level is up-regulated as the grade of the cell lines increase (Fig. 5*A*), suggesting a *TrkC-miR2*-positive expression relationship with grades of malignancy. *TrkC-miR2* expression level was also analyzed in CRC tumor samples compared with their non-tumor pairs. RT-qPCR results indicated an up-regulation of *TrkC-miR2* in CRC tissues (Fig. 5, *B–D*). Pathological tumor node metastasis (PTNM) staging and histopathological analysis indicated that *TrkC-miR2* expression was positively associated with different stages and grades of malignancy (Fig. 5, *D* and *E*). In other words, *TrkC-miR2* was expressed more in tumors with higher malignancy grade and advanced stage. Such an effect has been reported for some other tumor biomarkers (43). Furthermore, ROC curve analysis (44) evaluated the sensitivity and specificity of *TrkC-miR2* expression level for discrimination of CRC specimens (Fig. 5*F*). Analysis of *TrkC-miR2* and *APC2* target gene expression in the individual tumor samples suggested a negative correlation between them (Fig. 5, *G* and *I*). Then the Pearson correlation coefficient test confirmed a significant negative correlation between *TrkC-miR2* and *APC2* expression (Fig. 5*H*). Overall, accumulative evidence suggested that *TrkC-miR2* might be a *bona fide* biomarker for CRC diagnosis. Of course, analysis on a greater number of CRC samples is necessary to draw a confident conclusion.

Ectopic expression of TrkC-miR2 induces cell survival

Flow cytometry analysis, MTT assay, and crystal violet staining of the cells overexpressing *TrkC-miR2* indicated significant survival rate elevation of SW480 cells (Fig. 6). This effect was consistent with up-regulation of Wnt signaling (Fig. 4*A*) in SW480 cells overexpressing *TrkC-miR2*. The result is also in accordance with previously reported survival effect of *TrkC* (45, 46), which highlighted the effective cellular functionality of *TrkC-miR2* in parallel with *TrkC* host gene function. It has been reported that Wnt signaling pathway is active in the HUH7 cell line (47, 48). However, our analysis indicated that the Wnt pathway is not as strong as in SW480 cells (Fig. 4, *A* and *J*), probably due to the much higher expression level of *APC2* gene in HUH7 cells (supplemental Fig. 3*B*). That means a significant reduction of *APC2* transcript levels by *TrkC-miR2* overexpression in HUH7 cells (Fig. 4*H*) has not been critical for reduction of Wnt activity (Fig. 4, *I* and *J*). Accordingly, *TrkC-miR2* overexpression has not been able to affect the cell cycle status in HUH7 cells (Fig. 6*A*). Therefore, differential cell cycle effects of *TrkC-miR2* in HUH7 and SW480 cells could be attributed to different physiological conditions, and activity of the Wnt signaling pathway in transcript or protein levels, cell content, and genetics/epigenetics background (3, 5, 49) existed within the studied cell lines.

In conclusion, we here introduced *TrkC-miR2* as a functional miRNA mapped onto the 14th intron of *TrkC* gene together with accumulated evidence for its identity and oncogenic functionality against the components of Wnt signaling pathway, especially against *APC2* gene expression. The present evidence revealed a significant up-regulation of *TrkC-miR2* in CRC tumors and suggest it as a potential biomarker for CRC progression.

Experimental procedures

Bioinformatics prediction of miRNA and its candidate target genes

SSC profiler and miPRED bioinformatics tools were used to predict *bona fide* hairpin structures within *TrkC* gene. Drosha processing sites were predicted by using CID-miRNA software along with Microprocessor SVM program. *TrkC-miR2* and its precursor sequence conservation status were examined by using Mireval along with blat search against human genome and other organisms in UCSC database. MatureBayes, Pmirp, MiRNA Spotter, MiRmat, and MirZ online tools also predicted *TrkC-miR2*. The miRBase database was used to search for similar sequences of *TrkC-miR2* and its precursor in different species. RNAFOLD algorithm was used for prediction of RNA secondary structure. Potential target genes of *TrkC-miR2* were analyzed by RNAHybrid and DIANA-microT tools. Alibaba 2.1, P-Match, Tfsitescan, and Promoter2.0 Prediction Server bioinformatics tools were used for prediction of potential promoter sequences upstream of the putative stem-loop. To find the pathway in which *TrkC-miR2* is involved, DAVID (david-.abcc.ncifcrf.gov/), Diana-mirpath, and geneset2 miRNA online tools were applied. RNA-sequencing data were searched by using NCBI-SRA to examine the existence of novel discovered miRNAs in small RNA-sequencing data.

Cell lines

HCT116 and HT-29 cell lines were cultured in RPMI 1640 medium (Invitrogen), and SW480, HEK293t and HUH7 cell lines were cultured in DMEM-HG (Invitrogen). These media were supplemented with 100 units/ml penicillin, 100 μg/ml streptomycin (Sigma), and 10% fetal bovine serum (Invitrogen) and followed by incubation at 37 °C with 5% CO_2. HCT116 (ID# C570) and SW480 (ID# C506) cell lines were obtained from Pasteur Institute/Iran, and HEK293t (ID# IBRC C10683) and HT-29 (ID# IBRC C10097) were purchased from the National Center for Genetic and biological reserves in Iran.

Tissue samples

36 CRC tissue samples were obtained from Imam Khomeini and Dr. Shariati Hospitals, Tehran, Iran, and stored at −80 °C until used.

Table 1
Primer and oligo sequences that were used in the study

Primer name	Primer sequence, 5′ to 3′	Amplicon size (base pairs)
TrkC-real time	Forward, CCTGTGTCCTGTTGGTGGTTCTC Reverse, GAGTCATGCCAATGACCACAGTGTC	195
TrkC-premir2	GATTCTGAGCTGCACAGTCCAG	
TrkC-miR2-5p	GGCTGGGGATTCTGAGCT	
U48	Forward, TGACCCCAGGTAACTCTGAGTGTGT	
Anchored oligo (dT)	GCGTCGACTAGTACAACTCAAGGTTCTTCCAGTCACGACG (T)18V	
Universal-outer	GCGTCGACTAGTACAACTCAAG	
Universal-inner	AACTCAAGGTTCTTCCAGTCACG	
B-cat-real time	Forward, AGAACAGAGCCAATGGCTTG Reverse, CCTGGCCATATCCACCAGAG	130
c-myc-real time	Forward, CTCCTACGTTGCGGTCACAC Reverse, CGGGTCGCAGATGAAACTCT	142
GAPDH	Forward, GCCACATCGCTCAGACAC Reverse, GGCAACAATATCCACTTTACCAG	115
TrkC-Intron	Int-F: CTGGCGGCCGCTGAACAAGGGAGATGGCTCAGTGG Int-R: TAGACGCGTGGCTTTGCTGTCACCGCTGAGG	802
APC2-3′-UTR	Forward, GGGCGAAGCCTGTAATCACTGC Reverse, GAGTCGGACAGCTGACGGTG	2515
Axin1-3′-UTR	Forward, AAGGTGGACTGATAGGCTGGT Reverse, AGAAGACACACCACAGCCAGG	715
APC1-3′-UTR	Forward, TGGAACCCAAAGTCCTAAGC Reverse, CTGGGAAAACAACAGAAGTAG	2140
APC2-real time	Forward, TCCCAGCTCCCTGCCTCTGT Reverse, AGCCAGCCAGACCCAAGTTCT	129
APC1-real time	Forward, TATTACGGAATGTGTCCAGCTTG Reverse, CCACATGCATTACTGACTATTGTC	133
Axin1-real time	Forward, ATGCAGGAGAGCGTGCAGGTC Reverse, TGACGATGGATCGCCGTCCTC	237

DNA constructs

To clone the region corresponding to *TrkC-miR2* sense and antisense sequences, ~802 bp of human *TrkC*-intron-14 were PCR-amplified using Int-F and Int-R primers (Table 1) and cloned into pEGFP-C1 expression vector (Clontech) downstream of the GFP sequence both in sense and antisense directions. Human genomic DNA was extracted from white blood cells using standard protocol (50). A previously described hairpin structure sequence (51) was cloned into pEGFP-C1 vector as the scrambled control. TOP/FOP flash was also constructed into the pGL4 vector. All recombinant vectors were sequenced for verification of the correct insert.

Dual luciferase assay

Wild-type sequence of *APC2*3′-UTRs was cloned in psiCHECK vector downstream of luciferase gene for dual luciferase assay analysis according to its manufacture's protocol (Promega kit). Also, predicted MREs in this sequence were mutated, and amplified products were cloned in psiCHECK vector as negative controls (supplemental Fig. 1).

TOP/FOP flash assay

A TOP/FOP flash assay was used for Wnt signaling pathway analysis, and to this aim the TCF/LEF-responsive luciferase construct was made under the control of minimal TK promoter and tandem repeats of the TCF/LEF transcriptional response element (TRE). The cells were plated in 48-well plates and transfected with 400 ng of miRNA-encoding vector and with 200 ng of luciferase-encoding vector. The cells were harvested 48 h post-transfection, and luciferase activity was measured by using the Dual-Glo luciferase assay kit (Promega).

RNA preparation

Total RNA was isolated by using TRIzol (Invitrogen) according to the manufacturer's protocol and treated with RNase-free DNAaseI (Fermentas) and qualified on the agarose gel.

Primer designing

RT-qPCR was applied for detection of *TrkC-miR2* and its precursor and expression analysis of miRNA host and targets genes. Related primers were designed using NCBI Primer-blast (www.ncbi.nlm.nih.gov), IDT oligo analyzer, and MWG online PCR primer design tools. Primer and oligo sequences that were used in the study are listed in Table 1.

CDNA synthesis and RT-qPCR for detection of TrkC-miR2 and its precursor

CDNAs were made from polyadenylated RNAs according to the protocol (27), and each cDNA sample was amplified using specific primers in a real-time PCR system (Applied Biosystems) using the following conditions for 45 cycles: stage 1, 95 °C for 5 s; stage 2, 60 °C for 20 s; stage 3, 72 °C for 30s . RT-qPCR was performed according to Minimum Information for Publication of Quantitative Real-Time PCR Experiments (MIQE) guidelines using SYBRPremix Ex-TaqTM II PCR Mastermix (Takara, Japan) in experimental duplicates. Expression data were analyzed using endogenous *U48* and *GAPDH* as the reference genes and were normalized using the $2^{-\Delta Ct}$ and $2^{-\Delta\Delta Ct}$ methods (52).

Overexpression of TrkC-premir2 in cell lines

The pEGFP-C1 expression vector containing *TrkC-miR2* precursor (0.8 μg DNA) was engulfed in Lipofectamine 2000 (Invitrogen) and used for transfection of HEK293t, SW480, and

HUH7 cell lines. 24 h later GFP microscopy (by Nikon eclipse Te2000-s) ensured successful transfection.

Azacytidine treatment

Azacytidine dissolved in water (Sigma) was used for treatment of HCT116 cells with a final concentration of 10 μM for 48 h. Then total RNA was extracted from these cells and used for RT-qPCR analysis.

Small molecules treatment

SW480 cells were seeded in 48-well plates, and 30 h later IWP-2, PNU74654, and XAV932 small molecules were applied in concentrations of 5, 6, and 5 μM for 10 h, respectively. Then, after 8 h of starvation, interested genetic constructs were transfected to the cells, and media were refreshed after 6 h. Then again small molecules were applied to resume their inhibitory effects. 48 h after transfection, the cells were lysed, and TOP/FOP flash assays were performed.

Cell cycle analysis

Cells were transfected with overexpression cassettes of *TrkC-premir2* and anti-*TrkC-miR2* and were harvested 36 h after transfection and stained with propidium iodide. All of the samples were analyzed with a FACS Calibur flow cytometer using Cell Quest software (BD Biosciences).

MTT assay

HUH7 and SW480 cells (8000 cells/well) were plated in a 96-well plate in tetraplicate. After 24 h they were transfected by interested constructs engulfed with Lipofectamine 2000. 20 μl of 5 mg/ml MTT (Sigma) was added to each well 36 h post-transfection followed by further incubation at 37 °C for 4 h, after which the culture medium was removed, and 100 μl of DMSO (Sigma) was added to each well to dissolve the formazan crystals. A_{490} was measured with an ELISA Microplate Reader (Biotek) as a function of cell viability

Statistical analysis

RT-qPCR data were analyzed Using DataAssist software V3.0 (53). Other statistical analysis was performed with GraphPad Prism 5.04 (GraphPad, San Diego, CA). For flow cytometry studies, data showing the percent of cell population within the negative group and test group were compared by using the Repeated Measures analysis of variance test followed by the Bonferroni test using GraphPad. RT-qPCR data resulting from 36 CRC tissue samples were analyzed using an unpaired non-parametric Mann-Whitney test by treating tumor and non-tumor samples as two independent groups using GraphPad Prism and SPSS software.

Author contributions—S. D. and B. M. S. conceived and designed the experiments. S. D., A Y., H. N., and M. J. performed the experiments. S. D. and B. M. S. analyzed the data. B. M. S., S. J. M., and M. N. contributed the reagents, materials, and analysis tools. S. D. and B. M. S. wrote the paper.

Acknowledgments—We thank Dr. Saman Hosseinkhani, Dr. Masood Soleimani, and Ali Fasihi for kind advice.

References

1. Reichardt, L. F. (2006) Neurotrophin-regulated signalling pathways. *Philos. Trans. R. Soc. Lond. B. Biol. Sci.* **361,** 1545–1564
2. McGregor, L. M., McCune, B. K., Graff, J. R., McDowell, P. R., Romans, K. E., Yancopoulos, G. D., Ball, D. W., Baylin, S. B., and Nelkin, B. D. (1999) Roles of trk family neurotrophin receptors in medullary thyroid carcinoma development and progression. *Proc. Natl. Acad. Sci. U.S.A.* **96,** 4540–4545
3. Genevois, A.-L., Ichim, G., Coissieux, M.-M., Lambert, M.-P., Lavial, F., Goldschneider, D., Jarrosson-Wuilleme, L., Lepinasse, F., Gouysse, G., Herceg, Z., Scoazec, J. Y., Tauszig-Delamasure, S., and Mehlen, P. (2013) Dependence receptor TrkC is a putative colon cancer tumor suppressor. *Proc. Natl. Acad. Sci. U.S.A.* **110,** 3017–3022
4. Jin, W., Kim, G. M., Kim, M. S., Lim, M. H., Yun, C., Jeong, J., Nam, J.-S., and Kim, S.-J. (2010) TrkC plays an essential role in breast tumor growth and metastasis. *Carcinogenesis* **31,** 1939–1947
5. Luo, Y., Kaz, A. M., Kanngurn, S., Welsch, P., Morris, S. M., Wang, J., Lutterbaugh, J. D., Markowitz, S. D., and Grady, W. M. (2013) NTRK3 is a potential tumor suppressor gene commonly inactivated by epigenetic mechanisms in colorectal cancer. *PLoS Genet.* **9,** e1003552
6. Aranha, M. M., Santos, D. M., Solá, S., Steer, C. J., and Rodrigues, C. (2011) miR-34a regulates mouse neural stem cell differentiation. *PloS ONE* **6,** e21396
7. Krol, J., Loedige, I., and Filipowicz, W. (2010) The widespread regulation of microRNA biogenesis, function and decay. *Nat. Rev. Genet.* **11,** 597–610
8. Wang, Z. (2010) MicroRNA: a matter of life or death. *World J. Biol. Chem.* **1,** 41–54
9. Wang, Y., and Lee, C. G. (2009) MicroRNA and cancer: focus on apoptosis. *J. Cell. Mol. Med.* **13,** 12–23
10. Miranda, K. C., Huynh, T., Tay, Y., Ang, Y.-S., Tam, W.-L., Thomson, A. M., Lim, B., and Rigoutsos, I. (2006) A pattern-based method for the identification of MicroRNA binding sites and their corresponding heteroduplexes. *Cell* **126,** 1203–1217
11. Berezikov, E., Cuppen, E., and Plasterk, R. H. (2006) Approaches to microRNA discovery. *Nat. Genet.* **38,** S2–S7
12. Berezikov, E., Guryev, V., van de Belt, J., Wienholds, E., Plasterk, R. H., and Cuppen, E. (2005) Phylogenetic shadowing and computational identification of human microRNA genes. *Cell* **120,** 21–24
13. Ng, E. K., Chong, W. W., Jin, H., Lam, E. K., Shin, V. Y., Yu, J., Poon, T. C., Ng, S. S., and Sung, J. J. (2009) Differential expression of microRNAs in plasma of colorectal cancer patients: a potential marker for colorectal cancer screening. *Gut* **58,** 1375–1381
14. Suzuki, H., Watkins, D. N., Jair, K.-W., Schuebel, K. E., Markowitz, S. D., Chen, W. D., Pretlow, T. P., Yang, B., Akiyama, Y., Van Engeland, M., Toyota, M., Tokino, T., Hinoda, Y., Imai, K., Herman, J. G., and Baylin, S. B. (2004) Epigenetic inactivation of SFRP genes allows constitutive WNT signaling in colorectal cancer. *Nat. Genet.* **36,** 417–422
15. Bienz, M., and Clevers, H. (2000) Linking colorectal cancer to Wnt signaling. *Cell* **103,** 311–320
16. Yang, L., Belaguli, N., and Berger, D. H. (2009) MicroRNA and colorectal cancer. *World J. Surg.* **33,** 638–646
17. Slaby, O., Svoboda, M., Fabian, P., Smerdova, T., Knoflickova, D., Bednarikova, M., Nenutil, R., and Vyzula, R. (2007) Altered expression of miR-21, miR-31, miR-143, and miR-145 is related to clinicopathologic features of colorectal cancer. *Oncology* **72,** 397–402
18. Bandrés, E., Cubedo, E., Agirre, X., Malumbres, R., Zárate, R., Ramirez, N., Abajo, A., Navarro, A., Moreno, I., Monzó, M., and García-Foncillas, J. (2006) Identification by real-time PCR of 13 mature microRNAs differentially expressed in colorectal cancer and non-tumoral tissues. *Mol. Cancer* **5,** 29
19. Dokanehiifard, S., Soltani, B. M., Parsi, S., Hosseini, F., Javan, M., and Mowla, S. J. (2015) Experimental verification of a conserved intronic microRNA located in the human TrkC gene with a cell type-dependent apoptotic function. *Cell. Mol. Life Sci.* **72,** 2613–2625
20. Dalmay, T. (2008) MicroRNAs and cancer. *J. Intern. Med.* **263,** 366–375

21. Abbott, A. L., Alvarez-Saavedra, E., Miska, E. A., Lau, N. C., Bartel, D. P., Horvitz, H. R., and Ambros, V. (2005) The let-7 MicroRNA family members mir-48, mir-84, and mir-241 function together to regulate developmental timing in *Caenorhabditis elegans*. *Dev. Cell* **9,** 403–414
22. Gomes, C. P., Cho, J.-H., Hood, L., Franco, O. L., Pereira, R. W., and Wang, K. (2013) A review of computational tools in microRNA discovery. *Front. Genet.* **4,** 81
23. Hapner, S. J., Boeshore, K. L., Large, T. H., and Lefcort, F. (1998) Neural differentiation promoted by truncated trkC receptors in collaboration with p75 NTR. *Dev. Biol.* **201,** 90–100
24. Verdi, J. M., Birren, S. J., Ibáñez, C. F., Persson, H., Kaplan, D. R., Benedetti, M., Chao, M. V., and Anderson, D. J. (1994) p75 LNGFR regulates Trk signal transduction and NGF-induced neuronal differentiation in MAH cells. *Neuron* **12,** 733–745
25. Nishita, M., Hashimoto, M. K., Ogata, S., Laurent, M. N., Ueno, N., Shibuya, H., and Cho, K. W. (2000) Interaction between Wnt and TGF-β signalling pathways during formation of Spemann's organizer. *Nature* **403,** 781–785
26. Kunttas-Tatli, E., Zhou, M.-N., Zimmerman, S., Molinar, O., Zhouzheng, F., Carter, K., Kapur, M., Cheatle, A., Decal, R., and McCartney, B. M. (2012) Destruction complex function in the Wnt signaling pathway of *Drosophila* requires multiple interactions between adenomatous polyposis coli 2 and Armadillo. *Genetics* **190,** 1059–1075
27. Parsi, S., Soltani, B. M., Hosseini, E., Tousi, S. E., and Mowla, S. J. (2012) Experimental verification of a predicted intronic microRNA in human NGFR gene with a potential pro-apoptotic function. *PloS ONE* **7,** e35561
28. Li, B., Duan, H., Li, J., Deng, X. W., Yin, W., and Xia, X. (2013) Global identification of miRNAs and targets in *Populus euphratica* under salt stress. *Plant Mol. Biol.* **81,** 525–539
29. Neilsen, C. T., Goodall, G. J., and Bracken, C. P. (2012) IsomiRs: the overlooked repertoire in the dynamic microRNAome. *Trends Genet.* **28,** 544–549
30. McGahon, M. K., Yarham, J. M., Daly, A., Guduric-Fuchs, J., Ferguson, L. J., Simpson, D. A., and Collins, A. (2013) Distinctive profile of isomiR expression and novel microRNAs in rat heart left ventricle. *PloS ONE* **8,** e65809
31. Kalkman, H. O. (2009) Altered growth factor signaling pathways as the basis of aberrant stem cell maturation in schizophrenia. *Pharmacol. Ther.* **121,** 115–122
32. Nelson, W. J., and Nusse, R. (2004) Convergence of Wnt, β-catenin, and cadherin pathways. *Science* **303,** 1483–1487
33. Mosimann, C., Hausmann, G., and Basler, K. (2006) Parafibromin/hyrax activates Wnt/Wg target gene transcription by direct association with β-catenin/armadillo. *Cell* **125,** 327–341
34. Chen, B., Dodge, M. E., Tang, W., Lu, J., Ma, Z., Fan, C.-W., Wei, S., Hao, W., Kilgore, J., Williams, N. S., Roth, M. G., Amatruda, J. F., Chen, C., and Lum, L. (2009) Small molecule-mediated disruption of Wnt-dependent signaling in tissue regeneration and cancer. *Nat. Chem. Biol.* **5,** 100–107
35. Demilly, A., Steinmetz, P., Gazave, E., Marchand, L., and Vervoort, M. (2013) Involvement of the Wnt/β-catenin pathway in neurectoderm architecture in Platynereis dumerilii. *Nat. Commun.* **4,** 1915
36. Kahn, M. (2014) Can we safely target the WNT pathway? *Nat. Rev. Drug Discov.* **13,** 513–532
37. Bao, R., Christova, T., Song, S., Angers, S., Yan, X., and Attisano, L. (2012) Inhibition of tankyrases induces Axin stabilization and blocks Wnt signalling in breast cancer cells. *PloS ONE* **7,** e48670
38. Cammarata, P. R., Neelam, S., and Brooks, M. M. (2015) Inhibition of hypoxia inducible factor-1α down-regulates the expression of epithelial to mesenchymal transition early marker proteins without undermining cell survival in hypoxic lens epithelial cells. *Mol. Vis.* **21,** 1024–1035
39. Liu, J., Ding, X., Tang, J., Cao, Y., Hu, P., Zhou, F., Shan, X., Cai, X., Chen, Q., Ling, N., Zhang, B., Bi, Y., Chen, K., Ren, H., and Huang, A. (2011) Enhancement of canonical Wnt/β-catenin signaling activity by HCV core protein promotes cell growth of hepatocellular carcinoma cells. *PLoS ONE* **6,** e27496
40. Morin, P. J., Sparks, A. B., Korinek, V., Barker, N., Clevers, H., Vogelstein, B., and Kinzler, K. W. (1997) Activation of β-catenin-Tcf signaling in colon cancer by mutations in β-catenin or APC. *Science* **275,** 1787–1790
41. Kondoh, N., Schweinfest, C. W., Henderson, K. W., and Papas, T. S. (1992) Differential expression of S19 ribosomal protein, laminin-binding protein, and human lymphocyte antigen class I messenger RNAs associated with colon carcinoma progression and differentiation. *Cancer Res.* **52,** 791–796
42. McInroy, L., and Määttä, A. (2011) Plectin regulates invasiveness of SW480 colon carcinoma cells and is targeted to podosome-like adhesions in an isoform-specific manner. *Exp. Cell Res.* **317,** 2468–2478
43. Link, A., Balaguer, F., Shen, Y., Nagasaka, T., Lozano, J. J., Boland, C. R., and Goel, A. (2010) Fecal MicroRNAs as novel biomarkers for colon cancer screening. *Cancer Epidemiol. Biomarkers Prev.* **19,** 1766–1774
44. Hartwell, L., Mankoff, D., Paulovich, A., Ramsey, S., and Swisher, E. (2006) Cancer biomarkers: a systems approach. *Nat. Biotechnol.* **24,** 905–908
45. Kumar, S., Kahn, M. A., Dinh, L., and de Vellis, J. (1998) NT-3-mediated TrkC receptor activation promotes proliferation and cell survival of rodent progenitor oligodendrocyte cells in vitro and *in vivo*. *J. Neurosci. Res.* **54,** 754–765
46. Minichiello, L., and Klein, R. (1996) TrkB and TrkC neurotrophin receptors cooperate in promoting survival of hippocampal and cerebellar granule neurons. *Genes Dev.* **10,** 2849–2858
47. Xu, N., Shen, C., Luo, Y., Xia, L., Xue, F., Xia, Q., and Zhang, J. (2012) Upregulated miR-130a increases drug resistance by regulating RUNX3 and Wnt signaling in cisplatin-treated HCC cell. *Biochem. Biophys. Res. Commun.* **425,** 468–472
48. Zhang, Y., Wei, W., Cheng, N., Wang, K., Li, B., Jiang, X., and Sun, S. (2012) Hepatitis C virus-induced up-regulation of microRNA-155 promotes hepatocarcinogenesis by activating Wnt signaling. *Hepatology* **56,** 1631–1640
49. Zhu, S., Wu, H., Wu, F., Nie, D., Sheng, S., and Mo, Y.-Y. (2008) MicroRNA-21 targets tumor suppressor genes in invasion and metastasis. *Cell Res.* **18,** 350–359
50. Sambrook, J., Fritsch, E., and Maniatis, T. (1989) *Molecular Cloning: A Laboratory Manual*, Cold Spring Harbor Laboratory Press, Cold Spring Harbor, New York
51. Xu, N., Papagiannakopoulos, T., Pan, G., Thomson, J. A., and Kosik, K. S. (2009) MicroRNA-145 regulates OCT4, SOX2, and KLF4 and represses pluripotency in human embryonic stem cells. *Cell* **137,** 647–658
52. Livak, K. J., and Schmittgen, T. D. (2001) Analysis of relative gene expression data using real-time quantitative PCR and the $2^{-\Delta\Delta Ct}$ method. *Methods* **25,** 402–408
53. Mestdagh, P., Van Vlierberghe, P., De Weer, A., Muth, D., Westermann, F., Speleman, F., and Vandesompele, J. (2009) A novel and universal method for microRNA RT-qPCR data normalization. *Genome Biol.* **10,** R64